urban science

MDPI

Article

GeoAI-Enabled Accessibility–Environment–Equity Mapping of a Functional Urban–Rural Continuum

Irma Kveladze

Department of Sustainability and Planning, Aalborg University (AAU), A.C. Meyers Vænge 15, 2450 København, Denmark; ikv@plan.aau.dk

Abstract

Urban expansion, peri-urban growth, and evolving mobility service systems are reshaping the functional links between urban and rural areas. As these relationships become increasingly complex, conventional urban–rural classifications may underestimate the spatial differences in everyday accessibility, environmental conditions, and demographic exposure. To capture these interrelated dimensions, this study develops a GeoAI-enabled Accessibility–Environment–Equity (AEE) framework to analyse the urban–rural continuum as a multidimensional functional space. Using Odense municipality as a case study, the framework incorporates network accessibility indicators, environmental benefit and pressure proxies, and demographic exposure indicators within a hexagonal tessellation. The indicators are combined into a standardised AEE feature matrix, interpreted through a principal component analysis, and classified using Gaussian mixture modelling with posterior-probability uncertainty mapping. The resulting typology shows a distinct but non-uniform core–periphery gradient: the central areas exhibit high accessibility and population density but lower green space availability and higher environmental pressure proxies, while the peripheral areas are greener but less accessible by non-car modes. The benchmarking against single-domain reference classifications reveals that the functional typology is primarily shaped by accessibility and demographic density structures rather than by greenness alone. This study advances urban–rural continuum (URC) research by demonstrating how GeoAI-enabled workflows can identify functional transition zones and accessibility–environment mismatches, supporting more evidence-based planning for medium-sized European cities and their surrounding urban–rural transition zones.

Keywords: GeoAI; multimodal accessibility; functional vulnerability; spatial equity; urban–rural continuum

Check for updates

Academic Editors: Jin Wang, Zhifeng Wu and Shan Wei

Received: 5 June 2026
Revised: 11 August 2026
Accepted: 19 August 2026
Published: 1 September 2026

Copyright: © 2026 by the author. Licensee MDPI, Basel, Switzerland. This article is an open access article distributed under the terms and conditions of the Creative Commons Attribution (CC BY) license.

1. Introduction

Urban–rural continua are increasingly being shaped by urban restructuring, peri-urban growth, dispersed settlement patterns, demographic change, and the reorganisation of mobility and service systems [1–3]. These processes challenge the assumption that urban and rural conditions can be adequately represented as mutually exclusive territorial classes, instead pointing to spatial gradients where settlement morphology, accessibility, environmental benefits and exposure pressures, and demographic concentration interact [2,3]. This is particularly relevant for medium-sized European municipalities, where dense urban cores, suburban districts, peri-urban settlements, agricultural landscapes, and rural fringes often coexist within one functional planning territory [3–6]. In such settings, the key planning question is not only where people and buildings are concentrated, but how

different parts of the continuum function with respect to everyday accessibility and local environmental conditions [7,8].

Standardised urban–rural frameworks, including the OECD–European Commission approach to cities and functional urban areas and Eurostat's Degree of Urbanisation, provide essential tools for comparative monitoring by classifying territories according to their population density, settlement size, and contiguity [5,9,10]. Although suitable for international reporting, these morphology- and threshold-based schemes are not designed to represent fine-scale differences in walking and cycling access to daily services, first- and last-mile stop access, or local environmental benefit and exposure pressures [5,8,10]. As a result, places with similar density or land cover profiles may appear equivalent in conventional classes while differing substantially in everyday accessibility [5,11].

Accessibility is central to a functional reading of the continuum because it describes residents' ability to reach daily services and opportunities through transport and land use systems [12,13]. Sustainable and justice-oriented accessibility research emphasises that the opportunity for access should be understood in terms of mode, travel cost, destination type, and constrained mobility options, rather than Euclidean proximity alone [8,14]. This matters particularly in peri-urban and semi-rural areas, where residents may live relatively close to an urban centre yet remain car-dependent due to weak active-mode networks, dispersed services, or limited access to stops [5,8,15]. Environmental conditions form a second functional dimension. Peri-urban and rural-fringe areas are often associated with higher green and open space coverage, whereas central and corridor locations may have a concentration of built-up intensity and infrastructure-related exposure pressures [7,16,17]. An environmental advantage, however, does not automatically imply territorial well-being: the benefits and burdens can diverge spatially from the accessibility patterns, producing planning-relevant mismatches along the continuum [7,18,19].

Recent unsupervised and GeoAI-oriented studies have shown that data-driven typologies can reveal latent territorial configurations beyond fixed urban–rural thresholds [4,20–22]. Using GeoAI, Tonini et al. [4] redefined Swiss territorial typologies with self-organising maps and hierarchical clustering using demographic, socio-economic, and physical attributes; Tocchi et al. [20], on the other hand, identified Italian urban and rural settlement archetypes for a risk-oriented exposure and vulnerability analysis; and related principal component analysis (PCA) clustering applications have classified peri-urban or rural types near metropolitan areas [21,22]. These contributions have demonstrated the value of GeoAI and multidimensional unsupervised classification [23]. Nevertheless, deriving the clusters alone does not ensure that a typology integrates multimodal non-car accessibility with environmental composition, remains transparent under alternative modelling choices, or provides uncertainty-aware evidence for planning [24–27]. Accessibility, environmental quality, and socio-demographic disadvantages are still frequently analysed in separate streams, so cross-domain mismatches can remain under-specified in morphology-centred or single-domain assessments [4,7,8].

In this context, the present paper develops and applies a GeoAI-enabled spatial workflow for mapping the functional structure along the urban–rural continuum in Odense municipality, Denmark. The contribution of this study mainly lies in the methodological novelty of a transparent and reproducible integration of (i) network-based walking and cycling service accessibility; (ii) public transport stop access potential; and (iii) green-share and built-up/environmental exposure proxies within a common hexagonal feature space, followed by a principal component analysis for gradient interpretation, probabilistic Gaussian mixture typology derivation, K-means robustness benchmarking, and explicit membership uncertainty and scenario sensitivity diagnostics [24–28]. In this framing, "GeoAI-enabled" denotes interpretable geospatial machine learning and spatial integration

for planning analysis [25–27]. The Odense case is used because its urban core, suburban, peri-urban, and rural-fringe conditions coexist within one municipal planning framework, resulting in accessibility–environment mismatches that are particularly consequential for medium-sized European city-regions [2–4]. Thus, the paper addresses three research questions: (1) How do multimodal accessibility, environmental conditions, and demographic vulnerability vary along the urban–rural continuum in Odense? (2) To what extent can a GeoAI-derived AEE typology reveal the transition zones and functional mismatches that morphology-oriented classifications may under-represent? (3) Which accessibility, environmental, and demographic indicators structure the functional URC typology, and how can the results support more differentiated and evidence-based spatial planning?

Within the proposed AEE framework, the three dimensions are regarded as co-constitutive rather than additive. Accessibility encompasses non-car reach to daily opportunities; environmental proxies reflect local amenities and infrastructure-related pressures; and equity-oriented demographic exposure identifies where these conditions converge with denser or more age-sensitive populations. Their interaction is analytically fundamental: high accessibility may coincide with environmental burdens in compact urban cores, while green amenities can align with limited walking and transit access at the periphery, and demographic concentrations may intensify the planning significance of either mismatch. Consequently, AEE delineates spatial co-occurrence and functional transitions along the urban–rural continuum; it does not assert causal relationships between domains.

The remainder of the paper is organised as follows: the next section reviews the relevant literature on urban–rural continuum classification, accessibility, environmental inequality, and interpretable GeoAI for spatial typology development. It is followed by the methodology, which explains the data sources and the seven-stage workflow, from defining the spatial units and constructing indicators to the feature space preparation, PCA interpretation, Gaussian mixture modelling (GMM) typology derivation, and uncertainty and benchmark assessment. Section 4 presents the identified spatial patterns, PCA results, functional typology, and benchmarking outcomes for Odense. Section 5 discusses the findings in relation to the research questions, planning implications, methodological transferability, and limitations. Finally, the conclusion summarises the study's contributions and potential directions for future research.

2. Literature Review

2.1. From Morphological Urban–Rural Classes to Functional Continuum Typologies

Urban–rural classification has traditionally relied on population density, settlement size, built-up contiguity, land cover thresholds or administrative boundaries [9,19,29]. Such approaches remain important for comparative territorial monitoring, particularly in the OECD–European Commission framework and Eurostat's Degree of Urbanisation, which provide harmonised categories for distinguishing cities, towns, semi-dense areas and rural territories [5,9,10]. Although these frameworks provide internationally comparable representations of settlement morphology, they are not designed to capture all the fine-scale functional differences in everyday service access, transport connectivity, environmental conditions, and population exposure. This limitation is especially relevant for medium-sized European municipalities, where urban cores, suburban districts, peri-urban settlements and rural fringes may coexist within a single planning territory. Accordingly, recent research supports a shift from binary urban–rural classification toward multidimensional continuum thinking. For instance, Rajendran et al. [29] argue for a systems-based understanding of peri-urban and urban–rural futures, emphasising that urban and rural areas should be interpreted through interconnected social, environmental, and spatial processes rather than as separate territorial categories. This systems perspective supports the analysis of

medium-sized city-regions as interconnected urban–rural territories rather than as collections of predefined and mutually exclusive zones. Similarly, Tan et al. [19] approach peri-urban planning from a landscape perspective, emphasising the importance of land use transformation, ecological structure, and spatial transition. Their work supports the inclusion of green area distribution, built-up intensity, and environmental pressures within a broader interpretation of functional peri-urban transition.

Comparative methodological studies further demonstrate that urban–rural classifications differ according to the territorial relationships they are designed to represent. Cattaneo and Girgin [30], for example, distinguish classifications centred on settlement form, accessibility to urban centres, and inter-settlement connectivity. Their comparison shows that morphology-based classifications, accessibility-oriented catchments, and network-based city-region models provide complementary rather than interchangeable representations of urban–rural systems. Cattivelli [31] similarly shows that the delineation of urban, rural, and intermediate territories depends on the selected variables, spatial units, classification rules, and intended policy applications. These findings indicate that no single classification can represent every functional dimension of the urban–rural continuum and that the appropriateness of a typology must be assessed in relation to its analytical and planning purposes.

Beyond these conceptual and comparative frameworks, recent studies operationalise the urban–rural continuum through multidimensional indicators and unsupervised learning. Tonini et al. [4] use physical, demographic, and socio-economic variables to derive data-driven Swiss territorial types along the rural–urban continuum, demonstrating that unsupervised classification can reveal configurations that fixed density-based or administrative categories may not identify. Paumelle et al. [6] combine open geospatial data with a cluster analysis to construct multidimensional territorial profiles of France, illustrating the value of systematic indicator development for characterising local environments beyond single-domain categories. Together, these studies provide methodological support for treating the urban–rural continuum as a multidimensional, data-driven typology rather than solely as a morphology-based classification.

Hybrid approaches extend this logic by combining dimensionality reduction, machine learning-based similarity, and clustering. Jiang et al. [22], for example, develop an urban–rural integration typology for villages in the Xi'an metropolitan area using economic, social, spatial, and ecological indicators within an unsupervised random forest–PCA–PAM workflow. Tocchi et al. [20] use geographic, demographic, and socio-economic indicators to identify urban and rural settlement archetypes for an exposure- and vulnerability-oriented analysis, while explicitly considering the validity and interpretability of the resulting archetypes. These studies confirm that multidimensional typologies can support differentiated territorial interpretations, but they also show that the resulting classes depend on the indicator selection, spatial scale, analytical procedure, and substantive purpose of the classification.

Building on these developments, the proposed AEE framework addresses a distinct but complementary analytical purpose. It is not intended to replace harmonised morphology-based classifications, accessibility catchments, or regional settlement typologies. Instead, it functions as a fine-scale diagnostic framework for examining how walking and cycling service accessibility, public transport stop access, environmental amenity and pressure proxies, and equity-related demographic exposure combine within the same spatial units. Its distinctive value lies in keeping the three domains conceptually distinct during indicator construction and interpretation, identifying cross-domain mismatches, retaining probabilistic class membership, and comparing the integrated typology with morphology-oriented and single-domain alternatives. The AEE framework, therefore, complements existing

urban–rural classifications by focusing on local functional conditions and planning-relevant combinations that broader territorial classifications are not designed to represent.

2.2. Accessibility, Environmental Proxies and Equity-Related Demographic Exposure as AEE Dimensions

Accessibility is a key dimension of functional URC analysis as it links people, transport networks and everyday opportunities. Hansen's [12] foundational work conceptualised accessibility as the potential for interaction between origins and destinations, while Geurs and van Wee [13] further demonstrated that accessibility depends on land use patterns, transport systems, travel impedance and measurement choices. These perspectives support the use of network-based measures rather than simple Euclidean proximity, and therefore suggest that walking and cycling service accessibility, along with public transport stop access potential, operationalise how different parts of a city municipality might function in relation to non-car access along the URC.

Environmental conditions constitute the second substantive dimension of the AEE framework. In this context, Wolch et al. [7] identified important health and environmental benefits associated with urban green space while cautioning that greening does not automatically produce equitable outcomes. Terefe and Hou [16] further showed that the use and benefits of green spaces depend not only on their spatial availability but also on their accessibility, quality, safety, social characteristics, perceptions, and institutional conditions. Ramachandran et al. [17] conceptualised environmental inequality in terms of the uneven distribution of environmental benefits and pressures among social groups. These studies undoubtedly support examining environmental conditions together with accessibility and population exposure, but they also indicate that green-cover availability should not be equated with effective access, use, or environmental justice. Accordingly, the environmental domain is operationalised using proxies for green–blue amenities and exposure to major roads or built-up areas. These indicators describe specific land cover and infrastructure features, but do not provide a comprehensive measure of environmental quality, as they exclude factors like heat exposure, air pollution, noise, remotely sensed vegetation conditions, and other environmental processes. Their purpose is to identify the relative combinations of land cover amenities and infrastructure-related pressures that can later be compared with non-car service accessibility and demographic exposure.

Recent accessibility and transport justice studies have further clarified why accessibility should be linked to equity. For example, Pereira et al. [32] argued that transport equity should be evaluated in relation to people's capacity to reach opportunities, while Lucas [14] associated transport disadvantage with social exclusion. Moukouei et al. [33] developed justice-oriented accessibility frameworks grounded in transport costs, and Tahmasbi et al. [34] demonstrated how integrated accessibility can support sustainable mobility assessments. These studies showed that limited non-car accessibility becomes a more significant planning concern when it overlaps with demographic or social disadvantages.

Accordingly, within the proposed AEE framework, equity is treated as a normative planning dimension rather than as a condition measured directly through a single index. Its empirical representation in this application is limited to the population concentration and the demographic exposure or sensitivity variable. These variables identify where population exposure or chosen demographic sensitivities align with accessibility or environmental disadvantages, but do not provide a full measure of socio-economic deprivation, distributive equity, or vulnerability. The indicators used do not fully account for factors such as income, education, employment, household car availability, health, housing conditions, or other elements that may influence people's ability to respond to spatial disadvantages. Therefore, transport equity research differentiates between mapping the spatial distribution of accessibility and evaluating whether that distribution is fair across different population

groups. Thus, the purpose of AEE is not to treat the three domains as interchangeable or combine them into a single measure. Instead, the framework investigates where relative accessibility, environmental amenity–pressure conditions, and demographic exposure align, diverge, or create cross-domain mismatches. These conceptual distinctions shape the construction and interpretation of the feature space discussed in the following section.

2.3. GeoAI, Clustering and Uncertainty-Aware Typology Construction

Integrating accessibility, environmental, and demographic indicators creates a multidimensional geospatial feature space where individual indicators may be correlated, and cross-domain configurations may not be apparent from fixed thresholds or univariate maps. A principal component analysis (PCA) is useful in this context as it supports the interpretation of dominant multivariate gradients and variable loadings in complex spatial indicator sets, as described by Demšar et al. [35]. However, a conventional PCA does not model spatial dependence directly; rather, it identifies the covariance structure among variables whose component scores can subsequently be examined geographically. In this context, GeoAI provides a broader framework for integrating geospatial data, machine learning, spatial reasoning, and interpretable geographic outputs. Mai et al. [27] describe next-generation GeoAI as moving towards representation learning, spatial machine learning, geographic knowledge integration, and interpretable geospatial modelling. Marasinghe et al. [26], in turn, emphasise that responsible urban GeoAI should remain transparent, reproducible, and contextually relevant for planning. These perspectives indicate that the objective is not merely to generate clusters but to develop a functional URC typology whose data, assumptions, interpretation, robustness, and uncertainty can be examined explicitly.

Recent urban typology research further emphasises the importance of model stability, planning knowledge, and spatial structure in unsupervised classification. Li and Li [36] use clustering ensembles to identify built-form patterns that remain consistent across alternative algorithms and parameter settings, demonstrating the value of assessing consensus rather than relying on a single clustering solution. Li and Quan [28] combine planning knowledge with hierarchical and Gaussian mixture clustering to translate statistical components into planning-relevant urban block types. Their approach shows that cluster interpretation and consolidation should be treated as a documented human-in-the-loop procedure rather than as a fully automatic output.

Spatial clustering research also distinguishes post-classification smoothing from models in which neighbourhood relationships influence class estimation. D'Urso et al. [37], for example, introduce fuzzy clustering with spatial regularisation so that both attribute similarity and geographic relationships contribute to membership estimation. Recent spatially regularised Gaussian mixture developments similarly incorporate spatial structure into mixture estimation rather than modifying class labels only after fitting the model [38]. These approaches provide relevant methodological comparators for evaluating whether a territorial typology is stable, interpretable, and genuinely geography informed. The distinction is important for accurately positioning the current framework. In this implementation, geographic adjacency is utilised in post-classification diagnostics and map generalisation rather than being directly integrated into the Gaussian mixture modelling (GMM) likelihood. The workflow is therefore GeoAI-enabled through geospatial feature construction, probabilistic machine learning, spatial diagnostics, and geovisual interpretation, but the fitted GMM itself remains non-spatial.

Within this methodological context, GMM [28,38,39] is relevant as it represents the feature distribution as a weighted combination of latent multivariate components and provides posterior membership probabilities for each observation. Unlike hard partition methods, GMM can accommodate components with unequal dispersion and orientation, depending

on the selected covariance specification. Li and Quan [28] demonstrate the application of GMM to regular-grid urban form indicators, showing how probabilistic components can be interpreted as planning-relevant urban types. The statistical basis of the model is finite mixture estimation through the expectation–maximisation algorithm [28,38,39]. This probabilistic representation is relevant to URC analysis because observations fall within regions where component distributions overlap may not be unambiguously assigned to a latent component. Posterior probabilities identify the dominant membership while preserving information about model-based membership ambiguity. However, this quantity does not represent the total classification uncertainty: it excludes the uncertainty arising from source data, indicator construction, interpolation, accessibility assumptions, spatial resolution, variable selection, component number, and post-classification processing. Cells with high posterior ambiguity may indicate gradual functional transitions, overlapping profiles, weak component separation, or model misspecification. They should therefore be interpreted alongside indicator profiles, neighbouring classifications, and sensitivity analyses rather than automatically labelled as transition zones.

K-means clustering and agreement metrics provide a simpler hard partition benchmark against which the GMM solution can be compared. In this regard, Hubert and Arabie's [40] adjusted Rand index offers a formal measure for comparing alternative classifications. Such a comparison is important because an unsupervised typology has no predefined ground truth. By comparing the GMM typology with accessibility-only, environmental proxy-only, demographic exposure-only, morphology-oriented, and quintile-based classifications, the analysis assesses whether the AEE typology merely reproduces a single dominant gradient or captures a more integrated functional structure. Finally, geovisual analytics provides the interpretive bridge between computational classification and planning reasoning. Andrienko et al. [25] emphasise that geovisual analytics supports data exploration by combining computational pattern detection with human interpretation. This supports the manuscript's use of maps, PCA interpretation, and uncertainty surfaces as part of an interpretable AEE workflow.

Taken together, this literature indicates that an interpretable functional URC typology requires transparent indicator construction, explicit model assumptions, probabilistic interpretation, sensitivity assessment, and comparison with simpler alternatives. For instance, unsupervised learning has notable limitations in urban planning. First, interpretability is not guaranteed: PCA–GMM solutions partition a feature space without an external ground truth, so class labels depend on indicator choices, loadings, and expert interpretation rather than predefined territorial categories [4]. Second, the results are sensitive to variable selection and model parameters; different feature sets, weights, or component counts can alter the typology, necessitating stability checks and benchmarks before planning use. Third, reproducibility requires transparent data provenance, detailed parameter reporting, and shareable workflows; without these, similar GeoAI typologies cannot be reliably audited or transferred across cities [6]. Therefore, unsupervised AEE typologies are best viewed as exploratory, uncertainty-aware decision-support tools rather than definitive zoning frameworks. Accordingly, the study develops a GeoAI-enabled AEE workflow that integrates four indicator groups within a standardised hexagonal feature space: walking- and cycling-based accessibility to services; public transport stop access potential; proxies for environmental conditions, built-environment characteristics, and road exposure; and equity-related demographic exposure. A PCA is employed to interpret the multivariate gradients, while GMM is utilised to estimate the probabilistic components, accompanied by benchmark classifications and sensitivity diagnostics to evaluate model dependence. The contribution of this study lies in its integrated and uncertainty-aware analytical design, rather than in proposing a novel algorithm. Its structure is potentially transferable;

however, the variables, thresholds, spatial resolution, and typology interpretation require recalibration according to the data availability, settlement structure, transport networks, and planning context to facilitate replication in other medium-sized European city-regions.

3. Materials and Methods

This study develops and applies a GeoAI-enabled spatial workflow to map the functional structure of Odense municipality along the URC. Its novelty lies in the architectural workflow rather than the algorithm: it specifies how established methods are to be sequenced to integrate multimodal accessibility and environmental indicators within a consistent spatial framework and to derive interpretable functional types with explicit uncertainty diagnostics. Empirically, the analysis employs a 500 m hexagonal grid clipped to the municipal boundary. The methodological sequence includes: (i) defining the study area and analytical spatial units; (ii) acquiring and harmonising the network, service, land cover, and other layers; (iii) constructing the walking, cycling, and public transport stop access indicators alongside the green-share, built-up and environmental exposure proxies; (iv) assembling a cell-level feature matrix with missing-value treatment, redundancy screening, and standardisation; (v) conducting a PCA for gradient interpretation; (vi) applying GMM for probabilistic typology derivation, with the K-means retained as a robustness benchmark; and (vii) performing single-domain benchmarking, membership uncertainty mapping, and a scenario sensitivity assessment. The subsequent subsections elaborate on these stages and distinguish the interpretive steps for the classification.

3.1. Study Area and Spatial Unit

Odense municipality was chosen as it is a medium-sized Danish city-region that includes a dense urban core, suburban residential districts, peri-urban settlements, agricultural landscapes, green corridors, and rural fringes within a single municipal planning framework (Figure 1). This spatial configuration makes it suitable for examining whether traditional urban–rural classifications accurately reflect functional differences in accessibility, environmental quality, and socio-demographic needs.

The analysis was carried out using a regular 500 m hexagonal grid (n = 1539 cells) as the common analytical unit in an EPSG:25832, ETRS89/UTM zone 32N coordinate system. The grid provided a consistent spatial framework for integrating network-based accessibility indicators, environmental metrics, land use data, and demographic indicators. Employing a regular grid also diminished the reliance on administrative boundaries and facilitated comparison across urban, peri-urban, and semi-rural areas. The 500 m grid resolution was selected for its suitability for planning, taking into account spatial details of input data, neighbourhood-scale interpretation, demographic aggregation, privacy constraints, and computational feasibility. However, it should not be regarded as an empirically validated optimal resolution, as further research is necessary to examine how sensitive the resulting typology is to alternative resolutions (e.g., 250 m and 1000 m) to assess potential scale effects.

3.2. Data Sources and Indicator Construction

The analysis integrated the transport, environmental and demographic data into three AEE domains (Table 1). All datasets were harmonised to the common projected coordinate system and summarised within the municipality-clipped hexagonal grids. The data processing and analyses were carried out in Python 3.13.7 using OSMnx 2.1.0, NetworkX 3.6.1, NumPy 2.4.6, Pandas 2.3.3, GeoPandas 1.1.3, Shapely 2.1.2 and Matplotlib 3.10.9.

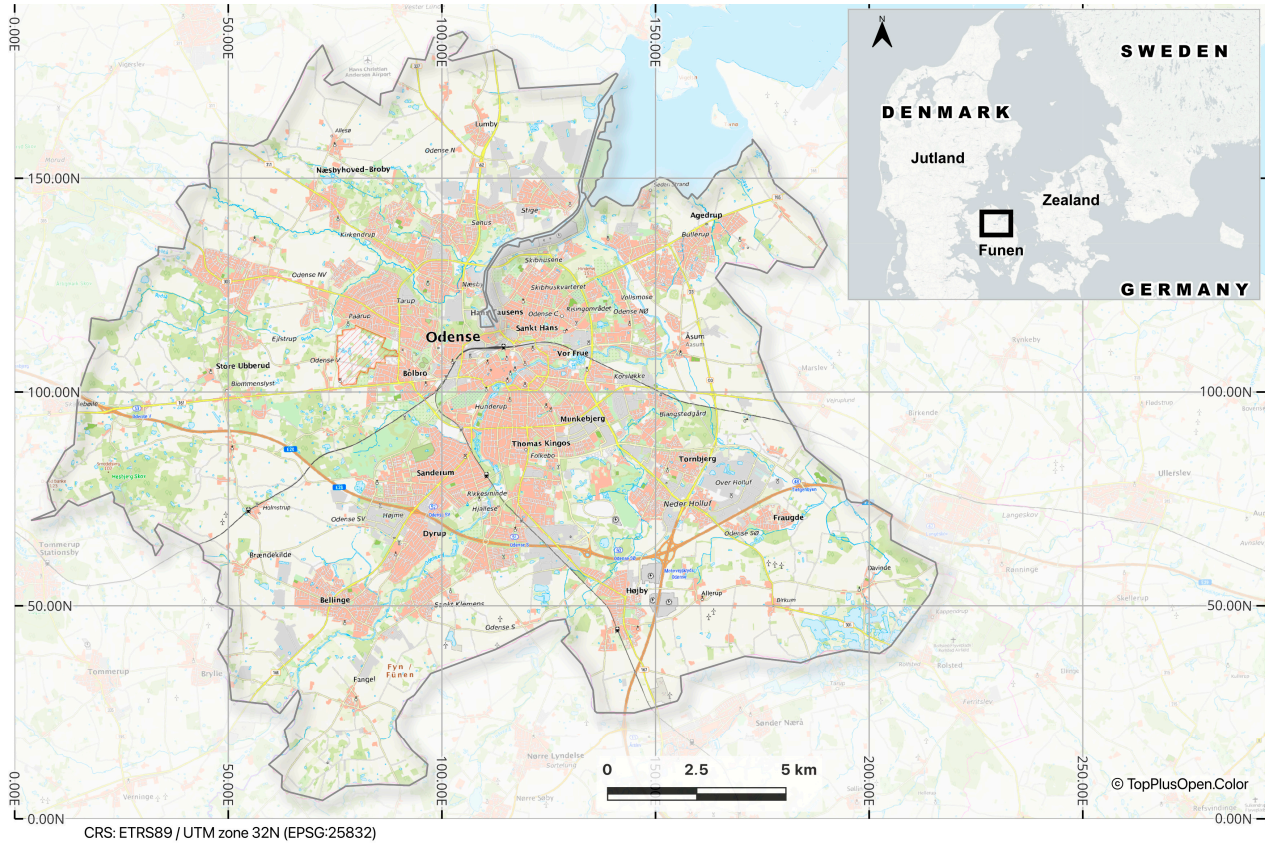


Figure 1. The map shows the location and spatial extent of Odense municipality in Denmark.

Table 1. Geospatial data and indicator groups used in the study. More details on metadata parameters are available at https://github.com/ikveladze/AEE_GeoAI-enabled_URC, accessed on 18 August 2026.

AEE Domain	Indicator Group	Operational Indicators	Source	Interpretation
Accessibility	Service accessibility	Shops, health, education, civic services, food/drink, recreation	OSM [41], Klimadatastyrelsen/Dataforsyningen geodata platform [42]	Network-based access to amenities/services
Accessibility	PT stop access	Stops/stations, walking access to PT nodes	OSM [41]/Klimadatastyrelsen/Dataforsyningen geodata platform [42]	First- and last-mile stop access potential
Environment	Environmental benefit proxies	Green areas, blue/green coverage, protected/open land, etc.	Klimadatastyrelsen/Dataforsyningen geodata platform [42]	Relative environmental benefit
Environment	Environmental pressure proxies	Built-up intensity, land use composition, major road exposure, etc.	Klimadatastyrelsen/Dataforsyningen geodata platform [42], Building and Housing Register (BBR) [43]	Relative environmental pressure
Equity	Demographic vulnerability proxy	Population density and available demographic sensitivity indicators	Statistics Denmark [44], Building and Housing Register (BBR) [43]	Relative demographic vulnerability

The time thresholds used in this study are literature- and planning-informed scenario settings for Odense's walk- and cycle-oriented everyday mobility context [45–47]; nested cycling (5/15 min) and PT (10/20 min) alternatives support the sensitivity comparison, while the typology uses the longer reference thresholds. The indicators were selected to operationalise the three AEE domains rather than through an automated feature search.

The accessibility indicators represent the everyday non-car service reach and first- and last-mile public transport stop access potential. The environmental indicators represent the amenity (green share and environmental quality) and settlement or infrastructure pressure (built-up share, major road exposure and environmental burden). The equity-related demographic indicators (population density and vulnerability composites) were constructed for mapping and interpretation. For the unsupervised typology derivation, the demographic vulnerability composites and the continuous functional URC score were excluded from the GMM inputs; nested short-threshold accessibility indicators (cycling 5 min; PT stop access 10 min) were retained for the profiling and sensitivity only.

Walking, cycling, and public transport stop accessibility were calculated as network-based, distance-decayed opportunity scores within mode-specific travel time thresholds, following established approaches [12,13,48]. The travel time thresholds were defined separately by mode: 15 min for walking, 5–15 min for cycling, and 10–20 min for PT stops (Table 2). The environmental domain captures both the benefits and pressure conditions, derived primarily from land cover and infrastructure information, supplemented by protected nature and supporting environmental surfaces [42]. The equity domain represents the population density and available demographic sensitivity indicators; these were used to interpret where accessibility or environmental disadvantages coincide with demographic exposure, not as full measures of distributive equity. These factors were included as accessibility disadvantages and have different planning implications depending on the social–demographic profile of the affected population [32,49,50].

Table 2. Comparison of modality indices.

Aspect	Walking	Cycling	PT stops
Network	Walk	Bike	Walk
Destinations	Service categories	Service categories	PT infrastructure categories
Speed	4.8 km/h	15 km/h	4.8 km/h
Thresholds	15 min	5–15 min	10–20 min
Decay β	700 m	1800 m	1000 m
Composite	Weighted services	Weighted services	50% stops & 50% weighted PT categories
Measured	Access to amenities	Access to amenities	Access to transit stops

Walking accessibility of amenities within each hexagon category was modelled using a cumulative opportunity approach based on the shortest path distance on the pedestrian network to the nearest service. Using a multi-source Dijkstra algorithm from NetworkX [51,52], the shortest path lengths were calculated from service nodes to reachable network nodes within a 15 min walking threshold, assuming a walking speed of 1.34 m/s (4.8 km/h) [53,54]. Distances were converted into category scores using the exponential decay $s(d) = \exp(-d/\beta)$, where d is the shortest-path network distance (m) and β is the mode-specific decay length. At $d = \beta$, $s(d) \approx 0.37$; thus, a larger β means slower decay and a longer effective accessibility range (Table 2). The category scores were combined into a weighted composite using fixed service category weights reflecting everyday necessities: food retail, 0.25; health, 0.20; education and childcare, 0.15; food and drink, 0.15; civic and daily services, 0.15; and recreation, 0.10. The hexagon scores were min–max scaled to 0–100 and mapped using a beyond-threshold class and quintiles across accessible cells [55]. Public transport accessibility followed the same walking network logic to OSM stops and stations (β = 1000 m; thresholds, 10 and 20 min) and combined all-stop proximity (0.5) with

a weighted PT category composite (0.5). This indicator measures the first- and last-mile stop access potential, not door-to-door, timetable-based public transport accessibility.

Cycling accessibility followed the same network accessibility logic as the bicycle network, with 5–15 min thresholds (15 km/h) and a larger distance decay parameter (β = 1800 m). Routing again relied on the multi-source Dijkstra algorithm in NetworkX, and the same service taxonomy and category weights as for walking were also applied.

The green-area share was calculated from official natural/green and land cover polygon features. The derived features were validated, clipped, dissolved, and intersected with each hexagon. The green share was then determined by dividing the intersected green area by the hexagon's total area. The classification was based on the municipality-wide quintiles of this green share.

The environmental conditions were summarised with a multi-source, cell-based model aligned to the hexagonal grid. The polygon features (green/natural cover, water, built-up classes, etc.) were overlaid and expressed as shares of cell area. The supporting surfaces for summer land surface temperature, state road noise, and road-related NO_2 proxy were included in the environmental quality and burden composites but were not used as separate GMM features. The positive components were normalised so that higher values indicated better conditions; the pressure components were normalised so that higher values indicated a greater burden. The available components were combined with transparent, normalised weights into environmental quality and environmental burden indices (0–100) and mapped to five relative classes. In the Odense implementation, the quality weights emphasise green/natural and protected land amenities, together with the inverse built-up and road exposure (supporting heat/noise relief where available). The burden weights emphasise low green/natural cover; the built-up intensity; road exposure; and supporting heat, noise, and air proxies (weights can be accessed via https://github.com/ikveladze/AEE_GeoAI-enabled_URC). The green/blue amenities and major road exposure are municipality-relative proxies for environmental advantages and infrastructural stress. These suffice for examining the correlation between non-car accessibility and local environmental conditions along the urban–rural continuum, not for absolute environmental health risks. In this study, they enable consistent cell-level comparisons using accessibility scores; however, they do not replace regulatory exposure assessments or health impact evaluations.

The demographic component allocated the Statistics Denmark zone counts to hexagons using a dasymetric approach: the parish population totals were redistributed with the BBR residential floor area weights, and soft-constrained against Statistics Denmark's population density classes and scaled to the municipal total. The age shares (0–14 to 65+) were derived from postcode-level age information using the same BBR weights. The population density and age composition were then combined into a demographic vulnerability index (0–100; relative classes). Socio-economic vulnerability indicators (education, unemployment, income) were unavailable in this data extract and therefore were not included in the composite (weights were renormalised to density and age). The density entered into the proposed typology only as a proxy for morphology/urbanity. The vulnerability indicators were retained for equity-oriented mapping and profiling and are excluded from GMM clustering.

The resulting indicators were subsequently screened, standardised, interpreted using PCA, and classified using GMM, as described in Sections 3.3–3.5 and shown in Figure 2. First, PCA was employed to interpret the dominant gradients in the AEE feature space. GMM was used as the primary clustering method because it provides probabilistic class membership, thereby supporting uncertainty mapping. The K-means was retained solely as a robustness benchmark. The final functional URC typology was derived from the GMM

solution and interpreted using cluster profile statistics. These steps are further described in more detail in the following sections.

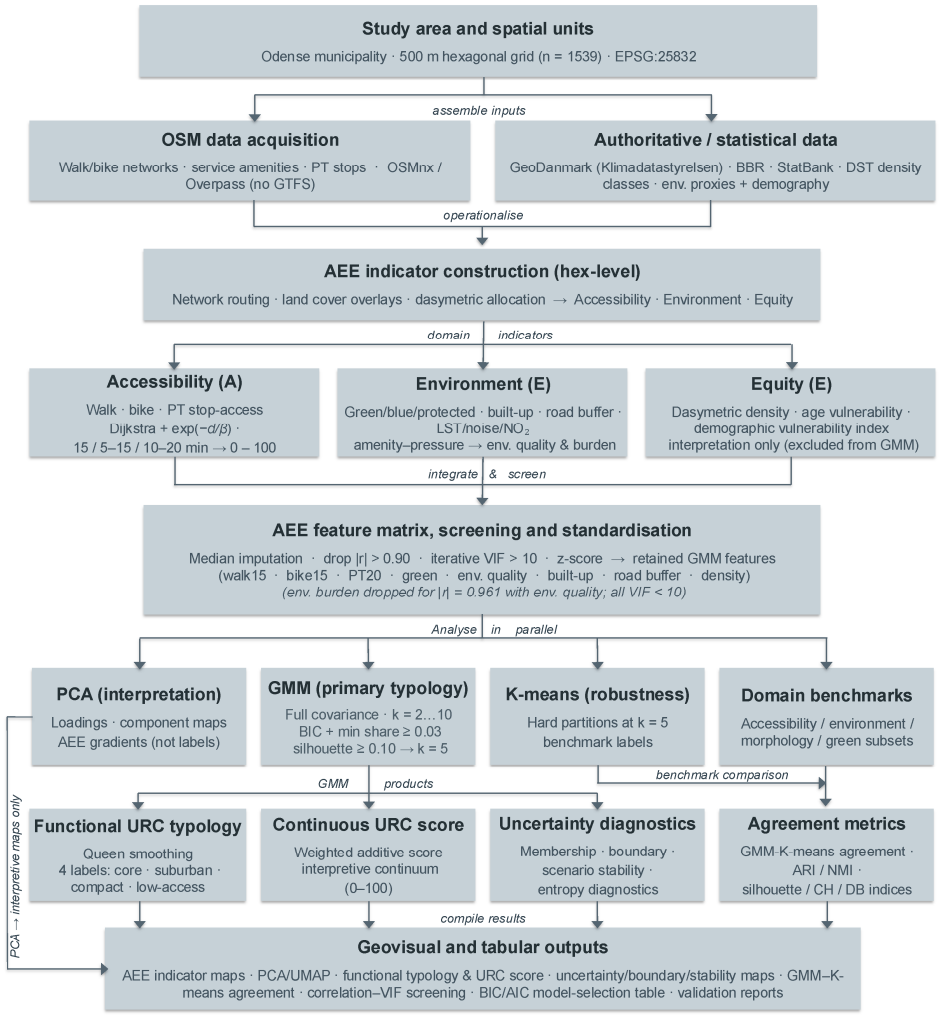


Figure 2. Methodological workflow for GeoAI-enabled functional URC mapping.

3.3. AEE Feature Space Construction and PCA-Based Interpretation

The AEE feature space was constructed by joining all indicators to the hexagonal grid using a common cell identifier. The broader standardised matrix used for the PCA interpretation included multimodal accessibility scores (including nested short thresholds), environmental shares and composites, supporting heat/noise/air means, population density and age vulnerability; the composite demographic vulnerability score and unavailable socioeconomic fields were excluded from this matrix. For the GMM typology derivation, the candidate inputs were further restricted to accessibility and environmental indicators, plus population density as a morphology proxy. Missing values were median-imputed. Redundancy was assessed using a pairwise Pearson correlation ($|r| > 0.90$; priority-preserving drop) and iterative Variance Inflation Factor (VIF) [56,57] screening (VIF > 10). The environmental burden was discarded due to collinearity with environmental quality ($|r| = 0.961$). The retained GMM feature set comprised walking accessibility (15 min), cycling accessibility (15 min), PT stop access (20 min), green share, environmental quality, built-up share, road buffer share and population density (all VIF < 10; maximum VIF ≈ 8.81). The Features were then z-score standardised so that no variable dominated solely because of the measurement scale; no additional unequal GMM feature weights were applied (correlation and VIF tables are available at https://github.com/ikveladze/AEE_GeoAI-enabled_URC). A PCA was

applied to the broader standardised AEE matrix to examine the dominant multivariate gradients along the URC [35]. The PCA was used as an interpretive step rather than as the final classification model. The component scores were mapped back to the hexagonal grid, and loadings were used to identify which indicators contributed most strongly to the observed variation.

For visual exploration, auxiliary K-means partitions [58] were applied in two ways: (i) to the first three principal component scores, supporting spatial interpretation of PCA structure; and (ii) to the full standardised AEE feature matrix, used to colour the PCA scatter plot. These partitions were exploratory only and were not used as the final GeoAI-derived URC typology. The final typology was derived from the GMM [39,59,60] fitted to the standardised AEE feature matrix, as described in the following section. In addition, UMAP [61] was applied for exploratory visualisation of local similarity in the standardised AEE feature space; the final functional typology was derived using GMM.

3.4. GeoAI-Enabled Functional URC Typology Derivation

The functional URC typology was derived from the median-imputed, z-score-standardised, nonredundant accessibility–environment–density feature matrix described in Section 3.3. Full-covariance GMMs were estimated for $k = 2, \ldots, 10$ (random_state = 42; n_init = 10) [28,39,59,60]. K was selected by minimising the Bayesian Information Criterion (BIC) among size-eligible models (minimum component share ≥ 0.03) that also met a silhouette preference ($\geq$0.10), yielding k = 5. The demographic vulnerability composites, nested short-threshold accessibility indicators and the continuous functional URC score were excluded from clustering [4,6,62]. Queen contiguity spatial weights [63] and majority smoothing [64,65] were applied to the GMM labels for visualisation coherence. The cluster profile statistics were used to interpret the five mixture components and assign four functional map labels: central accessible urban core; accessible suburban/local centre zone; compact built-up/environmental burden zone; and low-access transition zone. Separately, a continuous functional URC score (0–100) was computed as a weighted composite of low service accessibility (0.35), low population density (0.25), low built-up intensity (0.15) and green/environmental character (0.25); lower values indicated more urban/central conditions and higher values more rural/peripheral conditions. These continuum weights prioritised non-car service accessibility as the main functional differentiator, with the density, built-up intensity and green character as complementary rurality signals. The URC score was used for mapping and interpretation only and was not a GMM input. The GMM posterior probabilities were retained for an uncertainty assessment (Section 3.5). K-means [58,66] clustering with $k = 5$ components was run on the same screened feature matrix to serve as a robustness benchmark.

3.5. Benchmarking and Uncertainty Assessment

Benchmarking compared the four-type primary typology with (i) the quintile reference classes for the built-up intensity, green share, multimodal accessibility, environmental quality, continuous URC score and population density; and (ii) the single-domain or reduced-domain K-means solutions (k = 5) for accessibility-only, environment-only, morphology–density, and accessibility–environment feature subsets. An equity-only clustering benchmark was not retained since socio-economic vulnerability information was unavailable, and the demographic composite was excluded from the GMM. Agreement was assessed using cross-tabulations, class-mean indicator profiles, and the adjusted Rand index (ARI) and Normalised Mutual Information (NMI).

Uncertainty was evaluated at three levels: (1) the GMM membership uncertainty (1−maximum posterior probability), computed from the fitted mixture before spatial

smoothing; (2) the sensitivity across alternative feature subsets and neighbouring component counts, summarised with silhouette [66,67], Calinski–Harabasz and Davies–Bouldin indices [66,68,69] and with ARI/NMI [40,70,71] against the primary typology (scenario stability); and (3) algorithmic robustness via cell-wise agreement between the GMM and K-means hard labels on the same screened feature matrix [66]. Spatial uncertainty was mapped using Queen contiguity spatial weights [63–65] to derive the boundary heterogeneity. These diagnostics supported interpretation of soft transitions and model dependence; their implications for planning decisions are discussed in Section 5.

4. Results

4.1. Spatial Accessibility, Environmental Conditions, and Socio-Demographic Vulnerability

Across the municipality-clipped hexagon grid (n = 1539), the AEE indicators describe a strongly asymmetric urban fabric rather than a smooth centre–edge fade. The accessibility scores are right-skewed: the mean walking accessibility (15 min) is 14.6 (median 4.2), the mean cycling accessibility is 23.2 at 5 min and 37.7 at 15 min, and the mean PT stop accessibility is 21.5 at 10 min and 27.9 at 20 min. These municipality-wide averages are pulled upward by a compact high-access core, while large shares of the municipality remain outside everyday non-car catchments: 42.6% of cells fall beyond the 15 min walking cutoff; 39.9% beyond the 5 min cycling cutoff; and 64.3% and 40.9% beyond the 10 and 20 min stop access cutoffs, respectively. The environmental conditions are less extremely skewed but still uneven (mean green area share, 14.5%; environmental quality, 39.6; environmental burden, 49.9). The demographic vulnerability averages 10.0 (median 4.8), primarily reflecting the dasymetric density and age sensitivity, as the socio-economic vulnerability data were unavailable.

Figure 3 shows that this asymmetry is modality-specific, as each mode samples a different spatial process. Walking accessibility is tightly concentrated in the city centre and a few local centres [45]. The reason is structural: everyday services and a fine pedestrian network co-locate in a compact mixed-use fabric, so short walking thresholds reward density of destinations more than corridor connectivity. Once the amenity density thins, many cells drop abruptly below the 15 min threshold rather than declining gradually. Quantitatively, the cells in the top walking quintile average a walking score of 51.1 versus 1.5 in the bottom quintile, and they also show a much higher built-up share (69.3% versus 10.2%) and population density (≈2470 versus ≈100 persons km^{-2}). Cycling accessibility is broader and more continuous because the longer effective range allows the bicycle network to connect the residential belts to the same central and corridor-based service clusters; only 3.4% of cells remain beyond the 15 min cycling cutoff. Public transport stop accessibility follows a corridor-and-node logic: high values track with stop-rich central and arterial settings, while peripheral cells more often lack first- and last-mile stop access within 10–20 min of walking. In short, walking reveals proximity failure, cycling reveals network reach, and stop access reveals service geography rather than door-to-door timetable performance.

The environmental and demographic surfaces reverse parts of this gradient, creating a measurable accessibility–environment trade-off (Figures 3D and 4). The green area share and environmental quality increase towards the less built-up periphery, whereas the environmental burden and demographic vulnerability concentrate in the compact urban fabric. The same pattern appears in the mapped quintile classes and in the group-mean contrasts. The cells in the highest walking-accessibility quintile have, on average, a lower green share (10.6% versus 15.8%) and lower environmental quality (28.1 versus 44.1) than the cells in the lowest walking quintile, but a much higher environmental burden (66.0 versus 43.6), built-up share (69.3% versus 10.2%), population density (≈2470 versus ≈100 persons km^{-2})

and demographic vulnerability (23.9 versus 5.3). Green amenities and walking access are therefore not co-located across the grid: about 15% of cells combine above-median walking access with below-median green share, while about 17% combine below-median walking access with above-median green share. These contrasts are consistent with Figures 3 and 4 and quantify a classic mid-sized city sorting process: everyday services and denser housing concentrate where land is already built and more road exposed, while green amenities remain more abundant where development pressure and stop access supply are weaker.

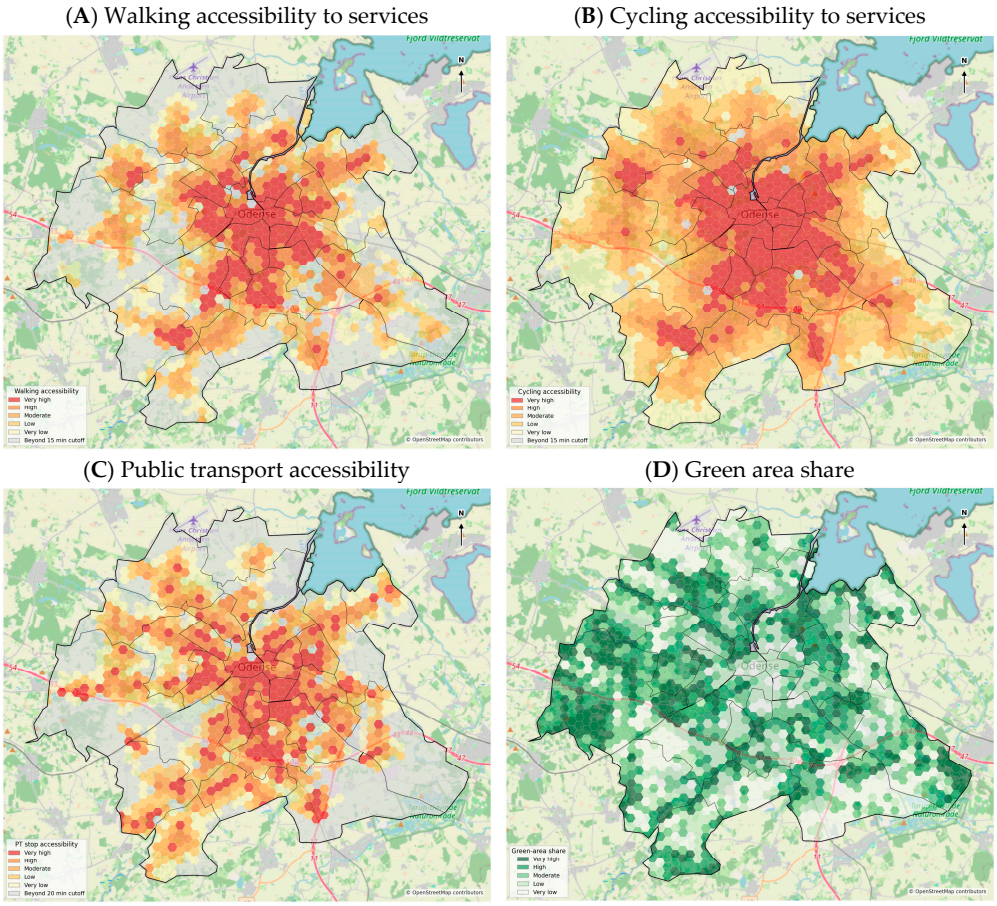


Figure 3. (**A**) Walking and (**B**) cycling accessibility with a 15 min network, (**C**) public transport accessibility with a 20 min network, and (**D**) green area share for Odense.

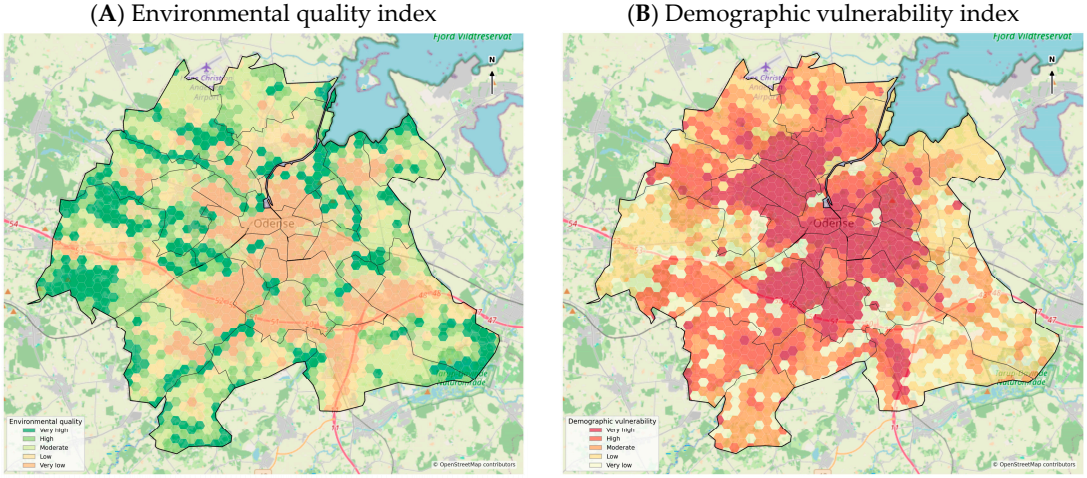


Figure 4. (**A**) Environmental and (**B**) demographic indicator maps.

For planning practice in mid-sized European municipalities such as Odense, three implications follow directly from these quantified patterns. First, walkability deficits outside the core are a destination access problem as much as a sidewalk problem: improving pedestrian conditions alone will have a limited effect unless everyday services are retained or inserted into suburban and outer local centres. Second, cycling is the most effective mobility option across the continuum because 15 min of cycling already covers most of the municipality; prioritising safe, continuous links from outer neighbourhoods to service clusters can reduce car dependence before full transit densification is feasible. Third, stop access gaps at the fringe, combined with a greener but service-poor periphery, call for coordinated first- and last-mile and local centre strategies rather than treating green provision and accessibility as separate agendas. In denser central cells, where vulnerability and environmental burden coincide with high access, planning should protect and provide green/blue areas without displacing the service mix that generates accessibility. In the low-access green periphery, the priority should be timed access to daily needs through local service nodes, feeder cycling, and stop placement, so that environmental amenities are not linked to mobility disadvantage.

4.2. Structure of the AEE Feature Space

PCA of the standardised AEE indicator matrix reveals a dominant continuum rather than discrete, well-separated clusters in the PC1–PC2 space (Figure 5). The PCA matrix includes multimodal accessibility scores, green/built and environmental quality–burden indicators, supporting heat (summer land surface temperature), air pollution and traffic noise surfaces, and population density and age vulnerability. PC1 explains 48.4% of the variance and PC2 15.9% (64.4% jointly; 74.0% for the first three components) (Figure 5). The loadings indicate that higher PC1 scores are associated with stronger multimodal accessibility, a higher built-up share and heat and environmental burden, and denser/age-sensitive contexts, whereas lower PC1 scores correspond to greener, higher environmental quality profiles. PC2 primarily distinguishes cells with stronger major road buffers and noise exposure (high PC2) from those with greener/higher-quality profiles (low PC2). As Figure 5 shows, the points form an elongated cloud along PC1, with a smaller high-PC2 extension of road- and noise-exposed cells rather than isolated class clusters. The colours also display the final four functional URC map labels from the BIC-selected five-component GMM (discussed in Section 4.3), overlaid on the PC scores to aid interpretation of where the typology classes sit along the continuum. They are not a separate K-means partition of the PCA plane. A hard K-means on the narrower-screened GMM feature set achieves a higher silhouette (≈0.40) than the selected GMM (≈0.11), which is expected: GMM is used to represent soft membership along the continuum, not to maximise hard cluster separation. The PCA view is therefore interpreted as evidence of a continuous functional urban–rural gradient that motivates a probabilistic typology rather than as a substitute for the map in Section 4.3.

4.3. GeoAI-Derived Functional URC Typology

A five-component GMM (k = 5), selected by BIC from the size-eligible solutions (minimum component share ≥ 0.03) with silhouette ≥ 0.10, was fitted to the screened, standardised clustering feature set (walking 15 min, cycling 15 min, PT stop access 20 min, green area share, environmental quality, built-up share, major road buffer exposure, and population density). The environmental burden was excluded prior to clustering due to near collinearity with environmental quality ($|r| = 0.961$). The demographic vulnerability composites and the continuous URC score were likewise excluded from the GMM inputs. Following Queen contiguity majority smoothing, the five components were interpreted as

four functional map labels (Figure 6). Spatially, the central accessible urban core (15.4% of cells; n = 237) is concentrated in central Odense and combines the highest multimodal accessibility (mean composite ≈ 0.61) with high built-up intensity and population density, but has comparatively low environmental quality (≈0.25) and a low mean URC score (≈41; 0 = urban/central, 100 = rural/peripheral). An accessible suburban/local centre zone (30.8%; n = 474) forms a broad intermediate belt with moderate accessibility (≈0.32), intermediate environmental quality (≈0.39), and a mean URC score of ≈62. A smaller, compact built-up/environmental burden zone (5.4%; n = 83) identifies road-exposed, compact fabrics with only moderate accessibility (≈0.24), low environmental quality (≈0.27), and elevated burden/road buffer exposure; its mean URC score (≈63) places it functionally between the suburban and low-access settings rather than in the urban core. The low-access transition zone is the most extensive class (48.4%; n = 745) and dominates the municipal periphery, combining the weakest accessibility (≈0.09) with the highest mean environmental quality (≈0.50) and the highest mean URC score (≈77).

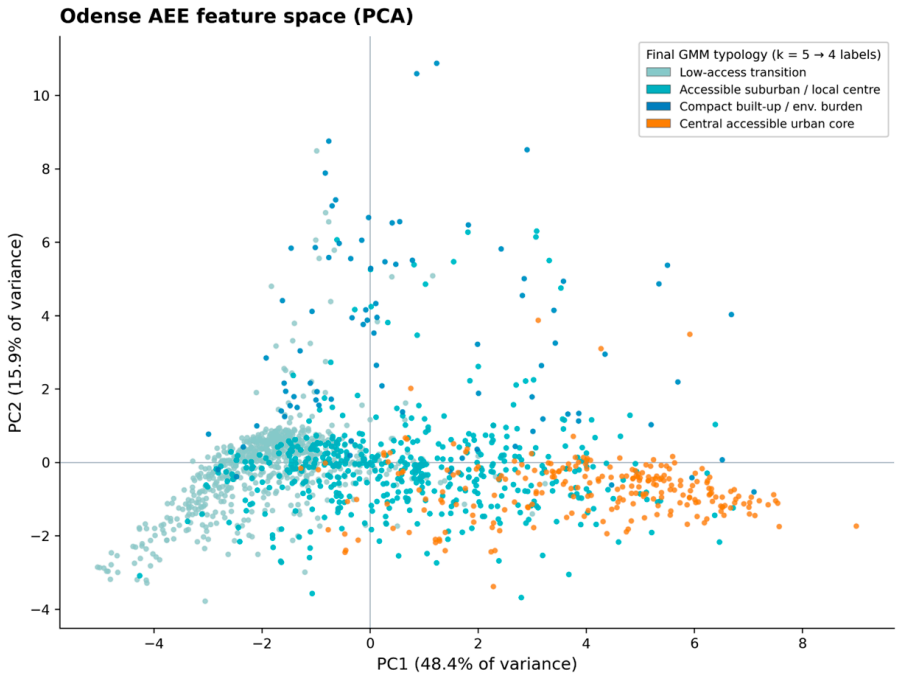


Figure 5. PCA representation of the Odense AEE feature space. Each point is a hexagonal cell (n = 1539). The PCA matrix comprises 15 median-imputed, standardised indicators: walking, cycling, and public transport stop accessibility; green area share, environmental quality and burden, built-up share, and major-road buffer exposure; supporting heat (summer land-surface temperature), air pollution, and traffic noise surfaces; and population density and age vulnerability. PC1 = 48.4% and PC2 = 15.9% of the variance (64.4% jointly). Colours show the final four functional URC map labels chosen from the BIC-selected five-component GMM after Queen smoothing (not exploratory K-means).

Cluster profiles, therefore, reveal a clear functional trade-off across the continuum: core and suburban cells extend service reach at the cost of local environmental amenities, while low-access peripheral cells reverse that pattern. The continuous URC score map in Figure 6A reinforces the same core–periphery gradient as a smooth surface rather than as a substitute for the typology. The contrast between the most urban and most rural quintiles of that continuous score clarifies the magnitude of the gradient. Compared to the highest-URC (most rural/peripheral) quintile, the lowest-URC (most urban/central) quintile has significantly higher scores for walking (47.2 versus 1.2), cycling (72.1 versus 14.9), and stop access scores (63.2 versus 5.2), but considerably lower green share (7.0% versus 37.0%)

and environmental quality (24.0 versus 58.1), along with higher burden (70.7 versus 31.3), built-up share (79.4% versus 3.0%), density (≈2780 versus ≈22 persons per km^2), and demographic vulnerability (24.9 versus 3.6). These contrasts quantify the same sorting process already evident in the typology and continuous score: services and denser housing cluster where land is already developed and more exposed to roads, whereas green amenities are more plentiful where development pressure and stop access supply are weaker.

(**A**) Functional URC score (**B**) GeoAI-derived functional URC typology

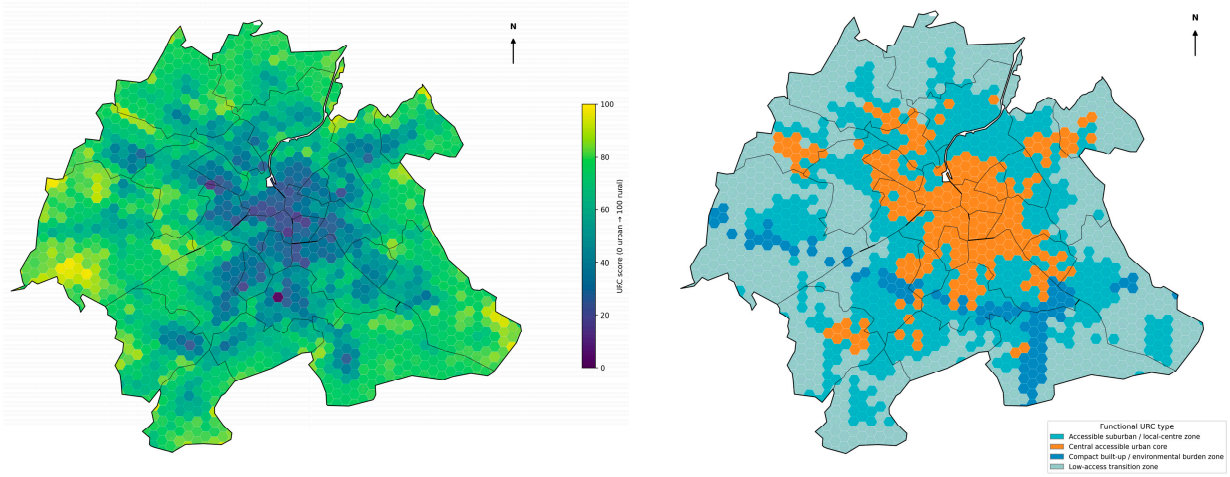


Figure 6. (**A**) The functional urban–rural continuum for Odense, based on a smoothed typology derived from AEE-based clustering, with a continuous URC score ranging from 0 (urban/central) to 100 (rural/peripheral). The classes serve as proxies for accessibility, environment, and equity rather than official zoning. (**B**) GeoAI-derived functional URC typology of Odense. GMM classes on the standardised AEE feature space, after spatial smoothing.

4.4. Uncertainty and Robustness of the Functional URC Classification

The GMM membership uncertainty was generally low (mean = 0.029; maximum ≈ 0.51), with higher values concentrated along class boundaries rather than in large contiguous interiors (Figure 7A). These cells mark soft functional transitions where the AEE indicators do not cleanly assign to a single component. The boundary heterogeneity based on the Queen contiguity averaged 0.32, indicating fragmented edges across the hexagonal tessellation (Figure 7B). The scenario stability across alternative feature subsets and neighbouring k settings averaged 0.57, suggesting moderate robustness overall, with residual sensitivity mainly in transition belts (Figure 7D).

An algorithmic comparison indicates partial agreement between the GMM and K-means hard labels (mean agreement ≈ 0.64 of cells; Figure 7C). On the screened clustering matrix, the K-means produces a clearer hard separation (silhouette ≈ 0.40) than GMM (silhouette ≈ 0.11), consistent with GMM's role as a soft typology model. The benchmark agreement with the final four-label typology is strongest for the accessibility-only and accessibility–environment clustering (ARI ≈ 0.29 and 0.28), moderate for the environment-only and morphology–density benchmarks (ARI ≈ 0.21 and 0.18), and weak for the green-share quintiles (ARI ≈ 0.02). The agreement with accessibility and URC score quintiles is also only moderate (ARI ≈ 0.20 and 0.19). The typology is therefore jointly structured by multimodal accessibility and settlement/density morphology and cannot be derived from greenness or environmental quality alone.

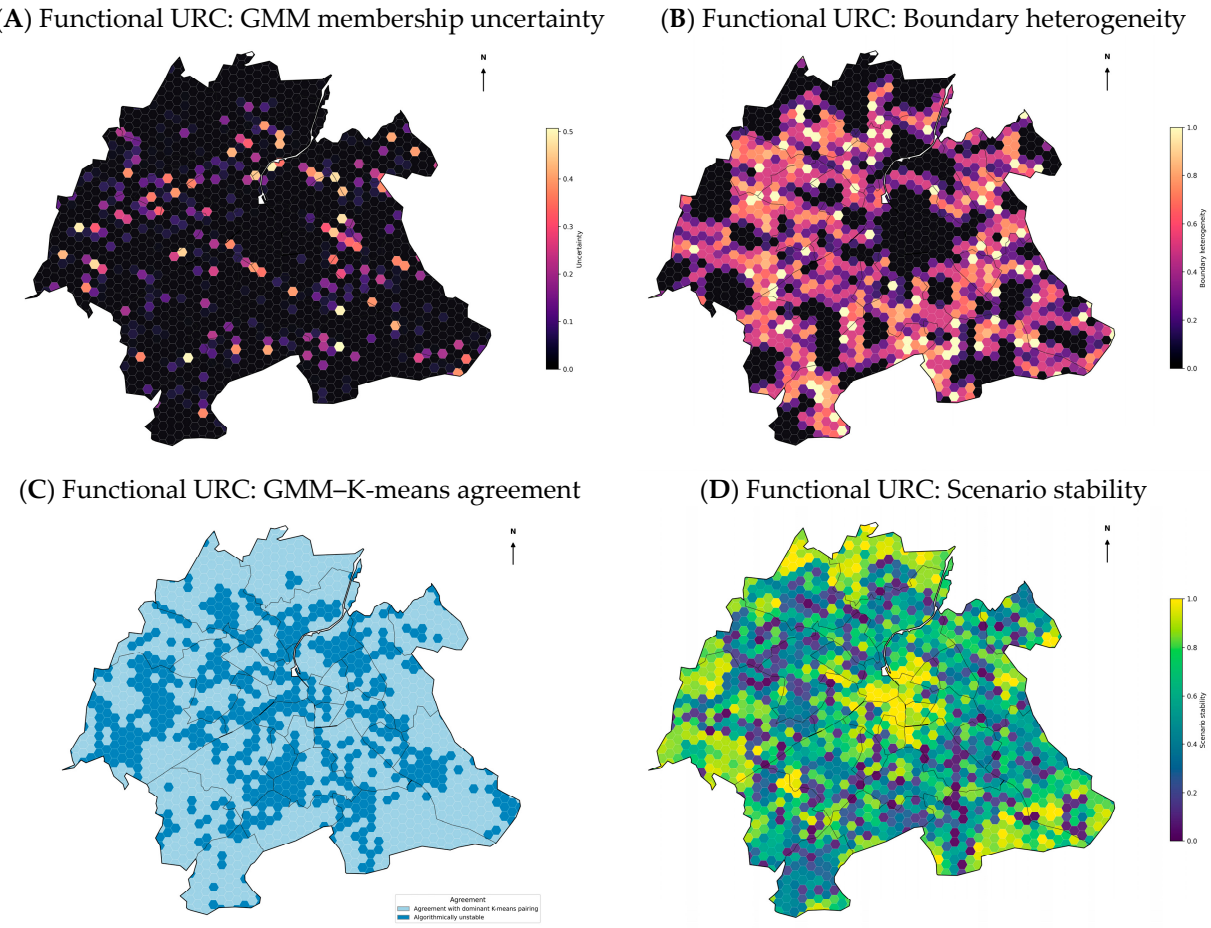


Figure 7. Robustness and uncertainty of the GeoAI-derived functional URC typology for Odense municipality: (**A**) GMM membership uncertainty; (**B**) boundary heterogeneity; (**C**) GMM–K-means agreement; and (**D**) scenario stability across feature subsets.

5. Discussion

Functional urban–rural structure beyond morphology—RQ1: The findings indicate that the URC constitutes a functional AEE configuration rather than a single morphological gradient [2,3,5,10]. Settlement centrality does not imply uniform everyday conditions. The central accessible urban core (~15% of cells) combines high non-car accessibility and density with a lower green share and higher environmental pressure. By contrast, the low-access transition zone (~48%) dominates the municipal periphery as a greener but service-poor area, while the accessible suburban/local centre (~31%) and compact built-up/burden (~5%) classes occupy intermediate positions that conventional "semi-urban" labels tend to flatten. These contrasts are also modality specific: walking is strongly centre concentrated, cycling is more continuous across the settlement system, and public transport stop access follows the nodes and corridors. Taken together, the pattern is consistent with accessibility as system-dependent opportunity [12,13] and with Wolch et al.'s caution that greening alone does not automatically produce equitable everyday outcomes [7].

Typology, mismatches and comparison with prior work—RQ2: The BIC-selected five-component GMM, interpreted as four map labels, highlights a key mismatch: environmental amenities and everyday non-car access are often disconnected. The greener fringe cells may remain functionally peripheral for walking and stop access, while high-access cores can be poor in amenities and more exposed to roads. The benchmarking supports this interpretation. The agreement with the green-share quintiles is minimal (ARI $\approx$ 0.02), while the accessibility-only and accessibility–environment solutions align

more closely (ARI ≈ 0.29 and 0.28). The morphology–density agreement is only moderate (≈0.18). Compared to the demography and land use/hierarchical typologies [4,21–23], the current solution is more organised around multimodal non-car reach and settlement density than greenness alone. Compared to planning-informed GMM of urban blocks [29], the municipal hexagon framework trades detailed design for broader coverage and explicit uncertainty in membership. Cattaneo and Girgin's distinctions between morphology, accessibility and network-centred classifications [31], along with Cattivelli's focus on the purpose-dependent typology choice [32], help explain why no single comparator reproduces the AEE map. In this context, Odense's class shares and local mismatches should be seen as case specific, while the staged PCA–GMM–benchmark–uncertainty sequence remains the key transferable feature. "GeoAI-enabled" here refers to an interpretable workflow—using established PCA, GMM and K-means methods [26–28]—rather than a new algorithm. The contribution lies in combining multimodal non-car accessibility with environmental proxies on a common grid, differentiating the interpretation from classification, and including uncertainty diagnostics in the assessment of typologies.

Organising indicators, proxies and planning implications—RQ3: Accessibility and settlement structures emerge as the primary organisers of functional space, while environmental conditions form a secondary contrast axis (PC1 ≈ 48.4%; PC2 ≈ 15.9%). For the research questions posed here, green/blue amenities and major road exposure are sufficient as municipality-relative amenity–pressure proxies because the analysis concerns the co-variation with non-car accessibility along the continuum, not absolute environmental health risk. Supporting heat, noise, and air surfaces enrich the composites where available, but they remain incomplete proxies. Multimodal accessibility should also be interpreted carefully: it denotes the joint interpretation of walking service access (15 min; β = 700 m), cycling service access (5/15 min; β = 1800 m), and PT stop access potential (10/20 min; β = 1000 m), not a single door-to-door travel time matrix. The PT indicator specifically measures the first- and last-mile walking access to mapped stops and stations; it does not include frequency, transfers, waiting, or in-vehicle times, so the conclusions are limited to the stop access potential. The cutoffs and β values are literature-informed distance-decay parameters and were not calibrated locally to behaviour. Although practical implications for mid-sized cities are already outlined in Section 4.1, it is still important to emphasise that, according to the Odense Kommuneplan, the green–blue structure [47] prioritises green–blue amenities and recreational continuity, yet the analysis shows that many of the greener peripheral cells remain weak regarding walking and stop access. Coordinating green structure goals with cycling, multimodal interchange, and collective transport, including Letbane feeder links, is therefore necessary if amenities are not to remain coupled with mobility disadvantage. High-access/low-green cores, by contrast, raise questions about liveability retrofitting. These remain diagnostic planning use cases rather than assessments of plan effectiveness.

Uncertainty and transferability: The uncertainty maps should be used in the same diagnostic manner. Three quantities must be distinguished: GMM membership uncertainty (soft component assignment prior to spatial smoothing), boundary heterogeneity (neighbourhood label fragmentation), and scenario stability (sensitivity to feature subsets and neighbouring k). The mean membership uncertainty is low (~0.029); however, the boundary heterogeneity (~0.32) and moderate scenario stability (~0.57) indicate that the edges remain method sensitive. The cells with low uncertainty and low heterogeneity may facilitate exploratory, class-specific screening. Conversely, the cells exhibiting high ambiguity or unstable boundaries should be regarded as functional transition zones. These zones require local corroboration through field knowledge and service audits and should not rely solely on the model for categorical zoning or investment decisions [26,27]. In

summary, the uncertainty surfaces serve as decision-support diagnostics: they indicate where labels are relatively robust and where planning judgment should remain provisional.

The same caution applies to the transferability. The staged workflow can be applied to other mid-sized municipalities, but only if they share a similar urban size, territorial characteristics, service hierarchy, network setup, data completeness, and demographic traits for analysis. The thresholds, weights, β parameters, and class labels need local adjustment, and municipality-relative scores are not universal standards across cities. Therefore, what is transferable is the analytical framework, not the Odense-specific classifications or policy suggestions.

Limitations and future work: Several limitations should be acknowledged when interpreting findings of this study. Firstly, "equity" is defined solely based on density and age-related demographic exposure; socio-economic variables were unavailable, and the vulnerability composite is omitted from GMM. Secondly, the analysis uses a single 500 m hexagon grid as a planning-oriented compromise between neighbourhood detail and municipal coverage. Complete recomputation at 250 m and 1000 m scales was not performed, leaving the MAUP and scale dependence unresolved, and it is not claimed that 500 m is empirically optimal. Finer grids would improve local detail but also add noise and fragmentation, while coarser grids would enhance municipal continuity at the expense of neighbourhood contrast. Thirdly, the environmental quality and burden are relative composites of amenities and pressures, mainly green/blue and built/road exposure, with supporting considerations for heat, noise, and air quality (NDVI and flood risk were not included), but not regulatory exposure or absolute environmental inequality. Fourthly, the PT measures only assess stop access potential, and the accessibility parameters lack calibration based on local behavioural data. Feature screening eliminated the highly collinear environmental burdens (Figure 2), yet the residual correlations among accessibility and built-up indicators mean caution is needed to avoid treating collinear gradients as independent drivers. Lastly, the unsupervised labels remain exploratory and depend on feature selection, the value of k, and the smoothing parameters; additionally, no external ground truth typology was available.

Future research should therefore broaden the current pipeline rather than analyse the existing maps in isolation. Priorities include recomputing at multiple grid resolutions, with the indicators reconstructed at each scale; using GTFS or official timetable matrices for comprehensive door-to-door PT analysis; calibrating the cutoff points and β parameters based on local behavioural data; incorporating richer socio-economic attributes; conducting longitudinal validation of functional transformations; making a careful comparison with spatial deep learning methods, considering interpretability and uncertainty; and integrating sensor and mobility datasets. Each of these extensions should involve rerunning the PCA, typology analysis, benchmarking, and uncertainty assessment within a unified workflow.

6. Conclusions

The study examines the URC in Odense as a functional AEE space rather than merely an administrative or morphological gradient. Multimodal non-car accessibility, comparative environmental conditions, and density and age-related demographic exposure systematically covary across the municipal hexagon grid; however, they do not move in tandem. High-access cores may be amenity-poor, whereas greener peripheral areas can remain deficient in access to walking amenities and PT stops. A probabilistic typology delineates these configurations more clearly than approaches based solely on greenness or morphology, indicating that the everyday functional structure within a mid-sized city is predominantly organised by non-car accessibility and settlement density, with environmental factors serving as secondary contrasts. Therefore, continuum mapping enhances the

value of planning by revealing such mismatches rather than reproducing a conventional urban–rural sequence.

The contribution of this work is not a novel algorithm but rather a transparent, uncertainty-aware, and planning-oriented spatial workflow. It integrates multimodal accessibility and environmental proxies within a reproducible pipeline comprising dimensionality reduction, probabilistic typology, and robustness diagnostics on a shared grid. When applied diagnostically, the outputs facilitate continuum-oriented screening of accessibility–amenity mismatches; however, they do not justify categorical policy decisions when membership remains ambiguous or scenario dependent.

The workflow architecture is transferable to other mid-sized municipalities, provided there are comparable levels of input completeness, network configuration, service hierarchy, and locally justified thresholds. Odense-specific class boundaries and municipality-relative scores are not portable; what is transferable is the staged analytical logic and the uncertainty reporting. The remaining limitations, such as the simplified demographic exposure, a single 500 m resolution, relative environmental proxies, and stop access rather than timetable-based public transport, bound the present claims and indicate the need for multi-resolution, GTFS-based, and socio-economically richer extensions within the same analytical pipeline.

Funding: This research received no external funding.

Data Availability Statement: The data, code, and derived results are available at: https://github.com/ikveladze/AEE_GeoAI-enabled_URC. Some datasets are not publicly available due to access or licensing restrictions and may be obtained from the original data providers under their applicable conditions.

Conflicts of Interest: The author declares no conflicts of interest.

References

1. OECD. *Rural Well-Being: Geography of Opportunities*; OECD Rural Studies; OECD Publishing: Paris, France, 2020.
2. Alexander Wandl, D.I.; Nadin, V.; Zonneveld, W.; Rooij, R. Beyond Urban–Rural Classifications: Characterising and Mapping Territories-in-between across Europe. *Landsc. Urban Plan.* **2014**, *130*, 50–63. [CrossRef]
3. ESPON—The European Observation Network for Territorial Development and Cohesion | ESPON. Available online: https://www.espon.eu/ (accessed on 28 April 2026).
4. Tonini, M.; Yu, J.; Hagen-Zanker, A. Redefining Swiss Territorial Typologies: An Unsupervised Learning Approach to the Rural–Urban Continuum. *J. Geovis. Spat. Anal.* **2025**, *9*, 24. [CrossRef]
5. OECD. *Getting to Services in Towns and Villages: Preparing Regions for Demographic Change*; OECD Rural Studies; OECD Publishing: Paris, France, 2024. [CrossRef]
6. Paumelle, M.; Occelli, F.; Wakim, L.M.; Brousmiche, D.; Bouhadj, L.; Ternynck, C.; Lanier, C.; Cuny, D.; Deram, A. Description of the Multi-Dimensional Environment at the Territorial Scale: A Holistic Framework Using Cluster Analysis and Open Data in France. *Ecol. Indic.* **2023**, *154*, 110562. [CrossRef]
7. Wolch, J.R.; Byrne, J.; Newell, J.P. Urban Green Space, Public Health, and Environmental Justice: The Challenge of Making Cities 'Just Green Enough'. *Landsc. Urban Plan.* **2014**, *125*, 234–244. [CrossRef]
8. Martens, K. *Transport Justice: Designing Fair Transportation Systems*; Routledge: New York, NY, USA, 2016. [CrossRef]
9. OECD; European Commission. *Cities in the World: A New Perspective on Urbanisation*; OECD Urban Studies; OECD Publishing: Paris, France, 2020. [CrossRef]
10. Eurostat. Review and Implementation of the Degree of Urbanisation. Available online: https://ec.europa.eu/eurostat/web/products-statistical-reports/w/ks-01-26-004 (accessed on 5 April 2026).
11. Páez, A.; Scott, D.M.; Morency, C. Measuring Accessibility: Positive and Normative Implementations of Various Accessibility Indicators. *J. Transp. Geogr.* **2012**, *25*, 141–153. [CrossRef]
12. Hansen, W.G. How Accessibility Shapes Land Use. *J. Am. Inst. Plan.* **1959**, *25*, 73–76. [CrossRef]
13. Geurs, K.T.; van Wee, B. Accessibility Evaluation of Land-Use and Transport Strategies: Review and Research Directions. *J. Transp. Geogr.* **2004**, *12*, 127–140. [CrossRef]
14. Lucas, K. Transport and Social Exclusion: Where Are We Now? *Transp. Policy* **2012**, *20*, 105–113. [CrossRef]
15. ITF. *Reversing Car Dependency: Summary and Conclusions*; ITF Roundtable Reports; OECD Publishing: Paris, France, 2021.

16. Endalew Terefe, A.; Hou, Y. Determinants Influencing the Accessibility and Use of Urban Green Spaces: A Review of Empirical Evidence. *City Environ. Interact.* **2024**, *24*, 100159. [CrossRef]
17. Ramachandran, S.; Rani, L.; Venkat, P. Exploring Environmental Inequality Definitions and Themes through Literature Review. *Discov. Sustain.* **2025**, *7*, 11. [CrossRef]
18. Robinson, M.; Bowring, J.; Davis, S.; Edwards, S. Spatial Opportunities at the Rural-Urban Fringe: Balancing Urban Growth, Food Production and Ecology. *Landsc. Res.* **2026**, *51*, 668–682. [CrossRef]
19. Tan, J.; Gu, K.; Zheng, Y. Peri-Urban Planning: A Landscape Perspective. *Plan. Theory* **2024**, *23*, 42–63. [CrossRef]
20. Tocchi, G.; Pittore, M.; Polese, M. Identifying Urban and Rural Settlement Archetypes: Clustering for Enhanced Risk-Oriented Exposure and Vulnerability Analysis. *Nat. Hazards Earth Syst. Sci.* **2025**, *25*, 3665–3692. [CrossRef]
21. Gonçalves, J.; Gomes, M.C.; Ezequiel, S.; Moreira, F.; Loupa-Ramos, I. Differentiating Peri-Urban Areas: A Transdisciplinary Approach towards a Typology. *Land Use Policy* **2017**, *63*, 331–341. [CrossRef]
22. Jiang, X.; Sun, J.; Zhang, T.; Li, Q.; Ma, Y.; Qu, W.; Ye, D.; Lei, Z. Defining Rural Types Nearby Large Cities from the Perspective of Urban–Rural Integration: A Case Study of Xi'an Metropolitan Area, China. *Land* **2025**, *14*, 602. [CrossRef]
23. Li, N.; Quan, S.J. Discovering Urban Block Typologies in Seoul: Combining Planning Knowledge and Unsupervised Machine Learning. *Cities* **2024**, *150*, 104988. [CrossRef]
24. Wang, J.; Biljecki, F. Unsupervised Machine Learning in Urban Studies: A Systematic Review of Applications. *Cities* **2022**, *129*, 103925. [CrossRef]
25. Andrienko, G.; Andrienko, N.; Jankowski, P.; Keim, D.; Kraak, M.J.; MacEachren, A.; Wrobel, S. Geovisual Analytics for Spatial Decision Support: Setting the Research Agenda. *Int. J. Geogr. Inf. Sci.* **2007**, *21*, 839–857. [CrossRef]
26. Marasinghe, R.; Yigitcanlar, T.; Mayere, S.; Washington, T.; Limb, M. Towards Responsible Urban Geospatial AI: Insights From the White and Grey Literatures. *J. Geovis. Spat. Anal.* **2024**, *8*, 24. [CrossRef]
27. Mai, G.; Xie, Y.; Jia, X.; Lao, N.; Rao, J.; Zhu, Q.; Liu, Z.; Chiang, Y.Y.; Jiao, J. Towards the next Generation of Geospatial Artificial Intelligence. *Int. J. Appl. Earth Obs. Geoinf.* **2025**, *136*, 104368. [CrossRef]
28. Li, N.; Quan, S.J. Identifying Urban Form Typologies in Seoul Using a New Gaussian Mixture Model-Based Clustering Framework. *Environ. Plan. B Urban Anal. City Sci.* **2023**, *50*, 2342–2358. [CrossRef]
29. Rajendran, L.P.; Raúl, L.; Chen, M.; Guerrero Andrade, J.C.; Akhtar, R.; Mngumi, L.E.; Chander, S.; Srinivas, S.; Roy, M.R. The 'Peri-Urban Turn': A Systems Thinking Approach for a Paradigm Shift in Reconceptualising Urban-Rural Futures in the Global South. *Habitat Int.* **2024**, *146*, 103041. [CrossRef]
30. Cattaneo, A.; Girgin, S. Beyond Urban and Rural: Exploring Form, Accessibility, and Interconnectivity in Global Urban Classifications. *npj Urban Sustain.* **2026**, *6*, 64. [CrossRef]
31. Cattivelli, V. Where Is the City? Where Is the Countryside? Assessing the Methods for the Classification of Urban, Rural, and Intermediate Areas in Europe. *J. Rural Stud.* **2024**, *109*, 103288. [CrossRef]
32. Pereira, R.H.M.; Schwanen, T.; Banister, D. Distributive Justice and Equity in Transportation. *Transp. Rev.* **2017**, *37*, 170–191. [CrossRef]
33. Moukouei, K.; Haghshenas, H.; Sahebgharani, A. Evaluating Justice in Accessibility to Urban Opportunities: Introducing Justice Analysis Frameworks Based on Theoretical Perspectives and Transportation Costs. *Sustain. Cities Soc.* **2025**, *118*, 106021. [CrossRef]
34. Tahmasbi, B.; Hajian, P.; Tahmasbi, F.; He, Q. Measuring Integrated Accessibility for Sustainable Mobility: A Fuzzy Set Approach Case Study. *Comput. Urban Sci.* **2024**, *4*, 35. [CrossRef]
35. Demšar, U.; Harris, P.; Brunsdon, C.; Fotheringham, A.S.; McLoone, S. Principal Component Analysis on Spatial Data: An Overview. *Ann. Assoc. Am. Geogr.* **2013**, *103*, 106–128. [CrossRef]
36. Li, J.; Li, C. Characterizing Urban Spatial Structure through Built Form Typologies: A New Framework Using Clustering Ensembles. *Land Use Policy* **2024**, *141*, 107166. [CrossRef]
37. D'Urso, P.; De Giovanni, L.; Federico, L.; Vitale, V. Fuzzy Clustering of Mixed Data with Spatial Regularization. *Spat. Stat.* **2025**, *65*, 100874. [CrossRef]
38. Sottosanti, A.; Risso, D.; Denti, F. Spatially Regularized Gaussian Mixtures for Clustering Spatial Transcriptomic Data. *J. Classif.* **2025**, *2025*, 1–23. [CrossRef]
39. Nagode, M.; Oman, S.; Klemenc, J.; Panić, B. Finite Mixture Models: A Key Tool for Reliability Analyses. *Mathematics* **2025**, *13*, 1605. [CrossRef]
40. Hubert, L.; Arabie, P. Comparing Partitions. *J. Classif.* **1985**, *2*, 193–218. [CrossRef]
41. OSM-OpenStreetMap. Available online: https://download.geofabrik.de/europe/denmark.html (accessed on 25 November 2025).
42. Dataforsyningen. Available online: https://dataforsyningen.dk/ (accessed on 28 June 2025).
43. Bygnings og Boligregistret (BBR) Forside—BBR Teknik. Available online: https://teknik.bbr.dk/forside (accessed on 28 April 2021).
44. Statistics Denmark Statistics Denmark. Available online: https://www.dst.dk/en/Statistik/emner/borgere/befolkning/befolkningstal (accessed on 18 January 2023).

45. Kveladze, I. Spatial Accessibility in the Urban Environment of a Medium-Sized City: A Case Study of Public Amenities in Odense, Denmark. *Urban Sci.* **2025**, *9*, 407. [CrossRef]
46. Moreno, C.; Allam, Z.; Chabaud, D.; Gall, C.; Pratlong, F. Introducing the "15-Minute City": Sustainability, Resilience and Place Identity in Future Post-Pandemic Cities. *Smart Cities* **2021**, *4*, 93–111. [CrossRef]
47. Byens Vision. Available online: https://www.odense.dk/byens-udvikling/byens-vision (accessed on 3 August 2026).
48. Boeing, G. OSMnx: New Methods for Acquiring, Constructing, Analyzing, and Visualizing Complex Street Networks. *Comput. Environ. Urban Syst.* **2017**, *65*, 126–139. [CrossRef]
49. Iamtrakul, P.; Chayphong, S.; Gao, W. Geospatial Analytics for Promoting a Healthy Peri-Urban City: A Health-Cartographic Perspective. *J. Urban Manag.* **2026**, *15*, 450–467. [CrossRef]
50. Liu, Q.; Zhe, T. Mapping the Evolution of Transport Justice Research: A Structural Topic Modelling Approach. *Transp. Policy* **2026**, *175*, 103898. [CrossRef]
51. Sniedovich, M. Dijkstra's Algorithm Revisited: The Dynamic Programming Connexion. *Control Cybern.* **2006**, *35*, 599–620.
52. Dijkstra, E.W. A Note on Two Problems in Connexion with Graphs. *Numer. Math.* **1959**, *1*, 269–271. [CrossRef]
53. Fossum, M.; Ryeng, E.O. The Walking Speed of Pedestrians on Various Pavement Surface Conditions during Winter. *Transp. Res. D Transp. Environ.* **2021**, *97*, 102934. [CrossRef]
54. Bosina, E.; Weidmann, U. Estimating Pedestrian Speed Using Aggregated Literature Data. *Phys. A Stat. Mech. Its Appl.* **2017**, *468*, 1–29. [CrossRef]
55. Zhou, Y.; Huang, X.; Li, Z.; Guo, Q.V.; Wei, H. Exponential Distance Decay in Urban Park Visitation: A Comparative Analysis of Recreational Mobility across 20 U.S. Metropolitan Areas. *Landsc. Urban Plan.* **2026**, *273*, 105690. [CrossRef]
56. O'Brien, R.M. A Caution Regarding Rules of Thumb for Variance Inflation Factors. *Qual. Quant.* **2007**, *41*, 673–690. [CrossRef]
57. Dormann, C.F.; Elith, J.; Bacher, S.; Buchmann, C.; Carl, G.; Carré, G.; Marquéz, J.R.G.; Gruber, B.; Lafourcade, B.; Leitão, P.J.; et al. Collinearity: A Review of Methods to Deal with It and a Simulation Study Evaluating Their Performance. *Ecography* **2013**, *36*, 27–46. [CrossRef]
58. MacQueen, J. Some Methods for Classification and Analysis of Multivariate Observations. In Proceedings of the 5th Berkley Symposium on Mathematical Statistics and Probability, Berkeley, CA, USA, 21 June–18 July 1967; Volume 5.1, pp. 281–298.
59. Dempster, A.P.; Laird, N.M.; Rubin, D.B. Maximum Likelihood from Incomplete Data Via the EM Algorithm. *J. R. Stat. Soc. Ser. B Stat. Methodol.* **1977**, *39*, 1–22. [CrossRef]
60. McLachlan, G.; Peel, D. Finite Mixture Models. *Annu. Rev. Stat. Its Appl.* **2000**, *6*, 355–378. [CrossRef]
61. McInnes, L.; Healy, J.; Melville, J. UMAP: Uniform Manifold Approximation and Projection for Dimension Reduction. *arXiv* **2018**, arXiv:1802.03426.
62. Leyerer, M.; Sonneberg, M.O.; Heumann, M.; Breitner, M.H. Decision Support for Sustainable and Resilience-Oriented Urban Parcel Delivery. *EURO J. Decis. Processes* **2019**, *7*, 267–300. [CrossRef]
63. Bivand, R.S.; Pebesma, E.; Gómez-Rubio, V. *Applied Spatial Data Analysis with R*, 2nd ed.; Springer: New York, NY, USA, 2013; pp. 1–405. [CrossRef]
64. Dong, R.; Dong, J.; Wu, G.; Deng, H. Optimization of Post-Classification Processing of High-Resolution Satellite Image: A Case Study. *Sci. China Ser. E Technol. Sci.* **2006**, *49*, 98–107. [CrossRef]
65. Huang, X.; Lu, Q.; Zhang, L.; Plaza, A. New Postprocessing Methods for Remote Sensing Image Classification: A Systematic Study. *IEEE Trans. Geosci. Remote Sens.* **2014**, *52*, 7140–7159. [CrossRef]
66. Sadeghi, B. Clustering in Geo-Data Science: Navigating Uncertainty to Select the Most Reliable Method. *Ore Geol. Rev.* **2025**, *181*, 106591. [CrossRef]
67. Rousseeuw, P.J. Silhouettes: A Graphical Aid to the Interpretation and Validation of Cluster Analysis. *J. Comput. Appl. Math.* **1987**, *20*, 53–65. [CrossRef]
68. Caliński, T.; Harabasz, J. A Dendrite Method for Cluster Analysis. *Commun. Stat. Theory Methods* **1974**, *3*, 1–27. [CrossRef]
69. Davies, D.L.; Bouldin, D.W. A Cluster Separation Measure. *IEEE Trans. Pattern Anal. Mach. Intell.* **1979**, *1*, 224–227. [CrossRef]
70. Strehl, A.; Ghosh, J. Cluster Ensembles—A Knowledge Reuse Framework for Combining Multiple Partitions. *J. Mach. Learn. Res.* **2003**, *3*, 583–617. Available online: https://dL.acm.org/doi/10.1162/153244303321897735 (accessed on 18 August 2026).
71. Vinh, N.X.; Epps, J.; Bailey, J. Information Theoretic Measures for Clusterings Comparison: Variants, Properties, Normalization and Correction for Chance. *J. Mach. Learn. Res.* **2010**, *11*, 2837–2854. Available online: https://dL.acm.org/doi/10.5555/1756006.1953024 (accessed on 18 August 2026).

Disclaimer/Publisher's Note: The statements, opinions and data contained in all publications are solely those of the individual author(s) and contributor(s) and not of MDPI and/or the editor(s). MDPI and/or the editor(s) disclaim responsibility for any injury to people or property resulting from any ideas, methods, instructions or products referred to in the content.